

CO adsorption on Pt induced Ge nanowires.

Danny E. P. Vanpoucke^{1,*} and Geert Brocks¹

¹*Computational Materials Science, Faculty of Science and Technology and MESA+ Institute for Nanotechnology, University of Twente, P.O. Box 217, 7500 AE Enschede, The Netherlands*

(Dated: May 16, 2022)

Using density functional theory, we investigate the possible adsorption sites of CO molecules on the recently discovered Pt induced Ge nanowires on Ge(001). Calculated scanning tunneling microscope (STM) images are compared to experimental STM images to identify the experimentally observed adsorption sites. The CO molecules are found to adsorb preferably onto the Pt atoms between the Ge nanowire dimer segments. This adsorption site places the CO molecule in between two nanowire dimers, pushing them outward, blocking the nearest equivalent adsorption sites. This explains the observed long-range repulsive interaction between CO molecules on these Pt induced nanowires.

PACS numbers: 73.30.+y, 73.61.-Ph, 68.43.-h

I. INTRODUCTION

In the last several decades, CO adsorption on Pt surfaces has been studied extensively both experimentally and theoretically. This large interest is partly due to the deceiving simplicity of the system and its industrial importance in catalytic processes, such as CO oxidation and Fischer-Tropsch synthesis.^{1,2}

However, a simple system such as CO adsorbed on the Pt(111)-surface, has and still does cause quite some controversy. Three decades ago, adsorption site preference and measured adsorption energies were the subject of discussion among experimental researchers. These problems have meanwhile been resolved and experimental results have converged to a coherent and detailed picture of this system.³⁻⁷ On the theorists side however, a discussion has emerged during the last decade regarding the unexpected failure of prevalent density functional theory (DFT) approximations to properly predict the CO/Pt(111) site preference. From experiment it is found that the ontop site is most stable in the low density regime, while local density approximation (LDA) and generalized gradient approximation (GGA) calculations show a preference for the threefold coordinated hollow adsorption site. The cause of this CO/Pt(111) puzzle seems to originate from the tendency of LDA and GGA to favor higher coordination and the flatness of the potential surface describing adsorption of CO on the Pt(111) surface.⁸ This has led to a search for better or alternative functionals in recent years.^{9,10}

Although the incorrect site prediction is a problem for DFT, this does not mean that the obtained geometries and derived physical properties are incorrect.¹¹ Even more, the calculated STM images derived from the geometries show excellent qualitative agreement with the experiment.^{12,13}

With the recent discovery of Pt induced nanowire (NW) arrays on Ge(001), a new Pt based adsorption surface becomes available.¹⁴ Decoration of these NWs with CO-molecules opens the way to the formation of one-dimensional (1D) molecular chains. Although the

adsorption of single CO-molecules on these Pt induced NWs has been observed experimentally, true molecular chains remain to be observed.^{15,16}

Room temperature (RT) STM experiments, by Öncel *et al.*¹⁵, showed the CO molecules to be very mobile along the NWs. Later, Kockmann *et al.*¹⁶ performed experiments at 70 K to suppress this mobility, and observed a long range repulsive interaction between pairs of CO molecules on the same NW. In those experiments the NWs were considered to be composed of Pt dimers in the troughs of a modified Ge(001) surface, called β -terrace,¹⁴ allowing for a straight forward interpretation of the observed STM images. The CO molecules were suggested to be adsorbed on the bridge positions of the NW dimers, comparable to the adsorption of CO on the Pt(001) surface.^{15,16}

Calculations on the interaction of CO with a free standing Pt monatomic wire suggest a similar behavior.¹⁷ However, in recent theoretical studies we showed the NWs to be modeled by Pt induced Ge NWs.^{18,19} In this model the NWs consist of Ge dimers placed in the Pt lined troughs of a Pt modified Ge(001) reconstructed surface. Since the sticking probability and affinity for CO on Ge is known to be low,²⁰ while being high for Pt, it would be surprising if CO molecules would adsorb on the Ge NW itself. This might lead to the suggestion that the theoretical models, proposed in Ref. 19, are in disagreement with the experiment. How can this theoretical model be reconciled with the experimental observations?

In this paper we study the adsorption of CO on Pt induced NWs, starting from the theoretical models we proposed previously in Ref. 18 and 19. Using *ab initio* DFT calculations, formation and adsorption energies are calculated. Theoretical STM images, generated using the Tersoff-Hamann method, are compared to experimental STM images to identify the adsorption sites and geometries observed in experiment.

This paper is structured as follows: In Sec. II the used theoretical methods are described. In Sec. III we present our results, which will be discussed more in depth in Sec. IV. Finally, in Sec. V the conclusions are given.

II. THEORETICAL METHOD

The calculations are performed within the DFT framework using the projector augmented waves method and the Ceperley-Alder LDA functional, as implemented in the VASP program.^{21–24} A 400 eV kinetic energy cutoff is applied for the plane wave basis set. CO molecules are placed on the models of both types of Pt induced NWs on Ge(001) we presented in Ref. 19. The surface/NW system is modeled by periodically repeated slabs of 12 layers of Ge atoms with NW reconstructions on both surfaces. A vacuum region of ~ 15.5 Å is used to separate the periodic images of the slab along the z axis. Due to the computational cost and the small size of the CO molecule a (2×4) surface cell for the solitary wire geometry, and a (4×4) surface cell for the array wire geometry is used. The Brillouin zone of the (2×4) ((4×4)) surface unit cell is sampled using a 8×4 (4×4) Monkhorst-Pack special k -point mesh.²⁵ To optimize the geometry of the surface/adsorbate system the conjugate gradient method is used while the positions of the Ge atoms in the center two layers are kept fixed as to represent the bulk of the system.

STM images are calculated using the Tersoff-Hamann method in its most basic form, with the STM tip approximated as a point-source.²⁶ The integrated local density of states (LDOS) is calculated as $\bar{\rho}(\mathbf{r}, \varepsilon) \propto \int_{\varepsilon}^{\varepsilon_F} \rho(\mathbf{r}, \varepsilon') d\varepsilon'$, with ε_F the fermi energy. Because the tunneling current is proportional to the integrated LDOS in the Tersoff-Hamann model, an STM-tip following a surface of constant current can be simulated through plotting a surface of constant (theoretical) LDOS: $\bar{\rho}(x, y, z, \varepsilon) = C$, with C a constant. For each C this construction returns a height z as a function of the position (x, y) . This heightmap is then mapped linearly onto a gray scale. The constant C is chosen such that the isosurface has a height z between 2 and 3 Å above the highest atom of the surface.

III. RESULTS

As is shown in literature, a small difference exists between solitary NWs (NW1) and NWs in arrays (NW2).²⁷ In experiment this difference presents itself as the appearance of a (4×1) periodicity at lower temperatures, which was traced back, in previous calculations, to the presence of an extra Pt atom bound to every pair of NW dimers.^{19,28} Since this extra Pt atom introduces new possible adsorption sites and geometries, CO adsorption on both NW geometries is studied.

Because some of the initial adsorption geometries relaxed into the same final structure, and because in some cases the geometry was modified extensively during relaxation, the adsorption sites presented in this manuscript are those found after relaxation.

The NW geometry is a metastable configuration and the adsorption of CO sometimes introduces large deformations of the surface. Therefore we define both a for-

mation and adsorption energy in these systems. The formation energy E_f indicates the energy gain/loss of the entire system due to the CO adsorption and the subsequent changes in the surface structure. It is defined (per (4×2) -surface unit cell) as:

$$E_f = (E_{\text{NW+CO}} - E_{\text{pristNW}} - N_{\text{CO}}E_{\text{CO}})/2, \quad (1)$$

with $E_{\text{NW+CO}}$ the total energy of the adsorbate-surface system, E_{pristNW} the total energy of a pristine slab + NW system and E_{CO} the total energy of a free CO molecule. N_{CO} is the number of CO molecules per surface unit in the system and the division by two is because CO is adsorbed at both faces of the slab. A negative value of the formation energy E_f indicates an increase in stability of the system. The adsorption energy E_{ad} refers to the binding energy of the CO molecule to the surface. Here any contribution due to surface deformation is excluded. It is defined (per CO molecule) as:

$$E_{ad} = (E_{\text{NW+CO}} - E_{\text{NW+sd}} - N_{\text{CO}}E_{\text{CO}})/(2N_{\text{CO}}), \quad (2)$$

with $E_{\text{NW+sd}}$ the total energy of the surface with the adsorption induced deformations but without adsorbed CO molecule.

A. CO on solitary NWs

Solitary NWs consist of Ge dimers located in the Pt lined troughs of a Pt modified Ge(001) surface. We will refer to this structure as NW1. Figure 1a shows the adsorption sites studied for this NW1 surface reconstruction. The adsorption and formation energies are given in Table I, as are some geometrical parameters, defined in Fig. 1c, for the CO molecule on the surface. The dimer length r_{CO} of a free CO molecule was calculated to be 1.1330 Å, in good agreement with the experimental value.²⁹ Table I shows the CO bond lengths are only slightly stretched in most cases: about 1.59–1.85%. The exception being CO adsorbed in the A3 configurations where the stretching is 13.95% and 7.15%. The difference between these last two configurations and the other configurations is the extra bond of the O atom with one of the surface atoms. In case of the A3a configuration the O atom has an extra bond with a Ge dimer atom [*cf.* Fig. 2a], while in the A3b configuration it is bound to a Pt atom of the top layer at the opposite side of the trough [*cf.* Fig. 2b]. Another interesting geometrical feature is that in most cases the adsorbed CO molecule is tilted with regard to the surface, unlike the behavior of CO molecules on clean Pt surfaces. In case of CO adsorbed on top of Pt atoms, the C-Pt bond length is just slightly longer than what is found for CO on Pt(111) in an atop configuration.^{1,30}

The adsorption energies given in Table I show a very clear preference for CO adsorption on Pt (sites A1–A4). The values of E_{ad} might indicate that CO also binds weakly to the Ge NW atoms (sites A5 and A6), contrary to the experimental knowledge that CO does not

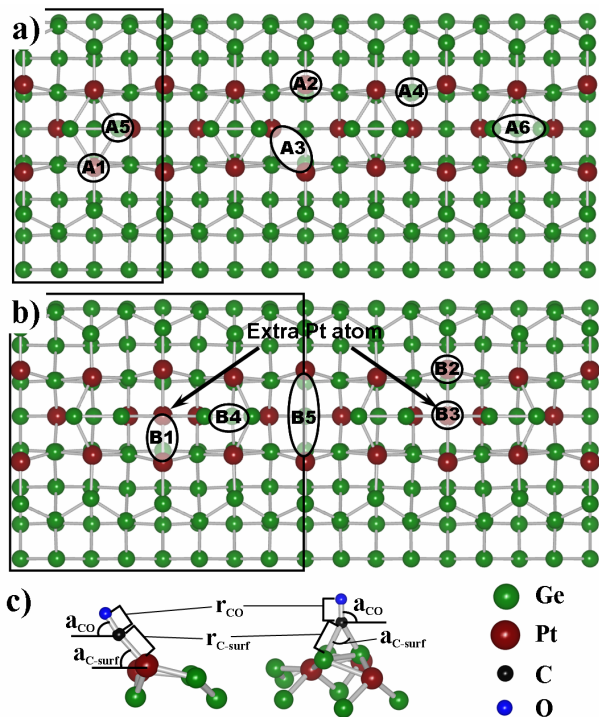


FIG. 1: (Color online) Adsorption sites of CO on a solitary NW geometry (a) and an array NW geometry (b). Green (red) balls indicate the positions of the germanium (platinum) atoms. Black rectangles indicate surface unit cells.

Adsorption energies and geometrical parameters
for CO on NW1.

	E_f (eV)	E_{ad} (eV)	coord.	r_{CO} (Å)	α_{CO} (°)	r_{C-surf} (Å)	α_{C-surf} (°)
NW1 A1	-1.300	-1.747	t	1.152	88	1.906	86
NW1 A2	-1.721	-1.990	t	1.154	57	1.920	48
NW1 A3a	-1.156	-0.993	b	1.291	56	2.246 (2.150)	117
NW1 A3b	-1.485	-2.069	b	1.214	47	2.012 (2.066)	101
NW1 A4	-2.859	-1.890	t	1.152	63	1.907	62
NW1 A5	-1.421	-0.439	t	1.151	70	2.015	70
NW1 A6	-0.349	-0.557	b	1.162	88	2.192	75

TABLE I: Formation and adsorption energies for CO adsorbed on the NW1-surface. Adsorption sites are shown in Fig. 1a. t (b) refers to top (bridge) adsorption. r_{CO} and r_{C-surf} are the C-O and C-Pt(Ge) bond lengths. For the A3 adsorption site the value between brackets is the C-Pt bond length between C and the Pt atom in the bottom of the trough. α_{CO} and α_{C-surf} are the bond angles with regard to the surface plane. In case of bridge adsorption α_{C-surf} is the angle between the two C-surface bonds. For the adsorption sites A1 to A4, the C atom is bound to surface Pt atoms, for the sites A5 and A6 the C atom is bound to Ge NW atoms.

bind to Ge. However, one needs to bare in mind that LDA tends to overbind, which in this case results in the small adsorption energies. Furthermore, the binding en-

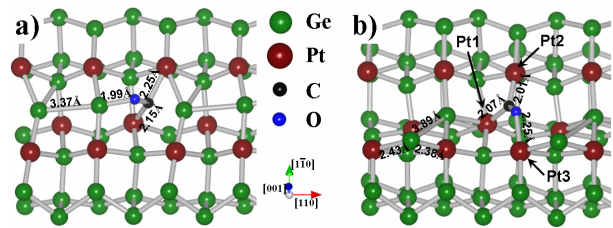


FIG. 2: (Color online) Ball-and-stick representations of the relaxed A3a (a) and A3b (b) adsorption structures.

ergies of CO on Ge are $E_{ad} \cong 0.5$ eV, while $E_{ad} \cong 2.0$ eV for CO adsorbed on Pt atoms, making the latter much more preferable.

The A3-structures are a bit peculiar, and, as we will show later, the A3a-structure results in calculated STM images that show extremely good agreement with the STM images obtained by Öncel *et al.*¹⁵ Both A3-structures have a bridge like adsorption geometry [*cf.* Fig. 2] but their adsorption energies differ more than 1 eV, making them the best and worst cases for CO adsorbed on the Pt atoms in this system. The most important contribution to the adsorption energy in this system comes from the CO bond-stretching. To examine the effects of this bond stretching, one can use a modified version of Eq. (2), replacing the formation energy of a relaxed gas molecule by the formation energy of a CO gas molecule with the same bond length as the adsorbed molecule. The resulting energy could then be considered the energy needed to desorb the molecule from the surface in a two step fashion. First, the bond(s) to the surface atoms are broken while the CO bond length remains unchanged. Then the molecule moves away from the surface relaxing to its equilibrium bond length. Since most adsorption geometries show only slightly stretched CO molecules, this energy only differs a little (~ 50 meV) from E_{ad} . However, for the strongly stretched A3-geometries a large difference with regard to E_{ad} is seen, resulting in energies of -2.010 eV and -2.384 eV for the A3a- and A3b-structures, respectively. This means that a CO molecule at an A3-site becomes the hardest to desorb from the surface using the path described above.

The somewhat peculiar adsorption geometry in case of the A3b-site can be understood when it is compared to the adsorption of CO on a monatomic Pt wire. In their theoretical study, Sclauzero *et al.*¹⁷ found that for an intermediate inter-platinum-distance of 3.7 – 5.3 Å a configuration with the CO molecule bridging the gap between two Pt atoms is the most stable configuration, while for an inter-platinum-distance around 2.50 Å the bridge configuration, with the C atom bound to two Pt atoms, was found to be most favorable. In the A3b-situation three Pt atoms are involved. Two (Pt1 and Pt2) are bound to the C atom and one (Pt3) is bound to the O atom. The distance between Pt1 and Pt2 is 3.145 Å, while the distance between Pt1 and Pt3, and Pt2 and Pt3 is 3.958 and

CO on the $4 \times$ NW1 surface cell.

	A1	A2	A3b	A4	A5	A6
E_f (eV)	-3.60	-3.58	-5.56	-2.72	-0.78	-1.35
E_{ad} (eV)	-1.94	-2.11	-2.00	-1.94	-0.67	-0.39

TABLE II: Adsorption and formation energies for the adsorption of one CO molecule per four NW dimers.

5.008 Å, respectively. Both the latter values are nicely in the intermediate range for the bridging configuration, while the former value lies in the range where Scлаuzero *et al.* found a simple bridge configuration to be most stable.

From Eqs. (1) and (2) follows that the energy due to the surface deformation induced by the adsorption of a CO molecule is given by: $E_{sd} = E_f - E_{ad}$. Positive values of E_{sd} indicate a destabilization due to the adsorbed CO molecule (A1, A2, A3b, and A6), while negative values indicate a stabilization (A3a, A4, and A5). In Ref. 19 the NW1-geometry was shown to be a metastable configuration. It was also shown that the adsorption configuration with the Ge NW dimer bound to four surface dimers (site C in Fig. 11a in Ref. 19) has a more favorable formation energy than the NW1 structure (*cf.* Table III in Ref. 19, compare γ_{as}^* Ge NW A (NW1) to γ_{as}^* Ge NW C).

This explains the increased surface stability seen for CO adsorption sites A3a, A4 and A5. From the large differences between the adsorption and formation energies, it is expected that adsorption of CO on the NW1-system has a large influence on the geometry of the wire, as can be seen for example in Fig. 2. Because the range of the (destructive) influence of a CO molecule on the wire is larger than the size of the used surface cell, some calculations are carried out using a surface cell $4 \times$ the unit cell length. Only a single CO molecule is absorbed on it, effectively reducing the CO density by a factor of four. Since the relaxation of such a huge cell is computational very demanding, lower accuracy relaxation parameters are used. E_f and E_{ad} are given in Table II showing even more clearly the effect of the CO molecule on the NW1 geometry

The large differences between E_f and E_{ad} again indicate large modifications of the NW1-structure. Comparing the relaxed geometries, we find that for larger differences between E_f and E_{ad} , more NW dimers are displaced or destroyed. In case of the A3b-structure even all four NW dimers are somehow modified. This behavior might be the basis of the experimentally observed long-ranged repulsive interaction between CO molecules.¹⁶ We will look into this aspect of CO adsorption in more detail in Sec. IV.

Adsorption energies and geometrical parameters for CO on NW2.

	E_f (eV)	E_{ad} (eV)	coord.	r_{CO} (Å)	a_{CO} (°)	r_{C-surf} (Å)	a_{C-surf} (°)
NW2 B1	-1.424	-2.336	b	1.171	76	2.086 (2.004)	82
NW2 B2	-0.761	-1.911	t	1.154	77	1.911	74
NW2 B3	-1.033	-2.090	t	1.155	90	1.868	90
NW2 B5	-0.784	-2.197	t	1.170	20	1.883	28
NW2 B4	-0.319	-0.916	b	1.163	62	2.003 (2.411)	72

TABLE III: Formation and adsorption energies for CO adsorbed on the NW2 surface. Adsorption sites are shown in Fig. 1b. t (b) refers to top (bridge) adsorption. In case of the B5 adsorption site, the C atom is bound to only one Pt atom, however, the O is bound to the Pt atom at the opposite side of the trough resulting in the entire CO molecule forming a bridge. r_{CO} and r_{C-surf} are the C-O and C-Pt(Ge) bond lengths. a_{CO} and a_{C-surf} are the bond angles with regard to the surface plane. For the B1 adsorption site the value between brackets is the C-Pt bond length between C and the Pt atom at the bottom of the trough. For the B4 adsorption site the value between brackets is the C-Ge bond length to the Ge atom bound to the extra Pt atom in the trough. In case of bridge adsorption a_{C-surf} is the angle between the two C-surface bonds. Only for the B4 site C is bound to Ge NW atoms, in all other cases C is bound to a Pt atom in the surface.

B. CO on NW-arrays

In Ref. 19 it was shown that the NWs in NW-arrays only differ very little from solitary NWs: a single extra Pt atom in the NW trough added to two NW1 unit cells, we will refer to this structure as NW2. The extra Pt atom (indicated in Fig. 1b) binds to two NW dimers, inducing the observed 4×1 periodicity. This extra bond also stabilizes the NW.^{19,31} Through its construction, the unit cell of a NW2 surface is twice the size of that of the NW1 surface and since we only adsorb 1 CO molecule per surface, this effectively halves the CO-coverage compared to that on the NW1 system.

Figure 2b shows the adsorption sites of CO on the NW2 4×4 surface cell after relaxation of the system.³² Only the adsorption sites different from those already present in the NW1-geometry, *i.e.* those where the extra Pt atom is involved directly or indirectly, are investigated. Our observations for the adsorption sites on the NW1-surface are assumed also to be valid for the equivalent sites on the NW2-surface.

The adsorption energies per CO molecule and the formation energies per 4×2 surface cell are shown in Table III. Just as for the the CO molecules adsorbed on Ge in the NW1 case, CO molecules adsorbed on Ge in the NW2 case (B4) have a much lower binding energy than CO molecules bound to Pt atoms, indicating the strong preference of CO toward Pt. The adsorption energies for CO molecules on Pt atoms are in the same range as for

the NW1-system, albeit slightly higher on average. This might be due to the lower CO coverage in the NW2-systems, reducing the direct and indirect interaction between CO molecules. The A2 and B2 adsorption sites, on the NW1- and NW2-geometries, respectively, differ only by the presence of the extra Pt atom, resulting in comparable adsorption energies. However, the presence of the extra Pt atom in case of the NW2-system prevents the CO molecule of bending far toward the surface, increasing the angle $\alpha_{\text{C-surf}}$ from 48° to 74° .

In case of the B5-site, where no extra Pt atom is present in the trough, the CO molecule bends very much toward the surface and actually bridges the through connecting two Pt atoms at opposing sides of the trough.

The distance between these Pt atoms is 4.826 \AA , placing them in the regime where Scлаuzero *et al.*¹⁷ found a “tilted bridge” configuration to be the energetically preferred configuration. In their study of CO adsorption on a freestanding monatomic Pt wire, Scлаuzero *et al.* identified 3 regimes for the CO adsorption geometry. i) For an unstretched (with Pt-Pt bond length $d_{\text{Pt-Pt}} = 2.34 \text{ \AA}$) freestanding Pt wire, the bridge configuration was found to be favored with respect to the ontop configuration by about 1 eV. The energy of the bridge configuration was shown to have a minimum for a value for $d_{\text{Pt-Pt}} = 2.50 \text{ \AA}$ just slightly above the equilibrium Pt bond length of the chain. We will refer to this as the unstretched regime. ii) In case of a hyperstretched configuration an energy minimum was found at $d_{\text{Pt-Pt}} = 5.05 \text{ \AA}$. In this case the substitutional geometry was found to be more favorable than the bridge configuration. In the substitutional configuration the CO molecule is aligned parallel with the Pt wire, and the C and O atom are bound each to a half of the Pt wire. iii) However, Scлаuzero and his collaborators found the energy minimum of the substitutional geometry to be still slightly higher than the tilted bridge configuration. In this tilted bridge configuration the CO bond lies in a plane through the wire, but it is not aligned parallel or orthogonal to the wire. Although no energy minimum for this configuration was found, Scлаuzero *et al.* found it to be preferred over the bridge and substitutional configuration for intermediate stretching lengths of the Pt-Pt distance (about $3.8 \text{ \AA} \leq d_{\text{Pt-Pt}} \leq 5.1 \text{ \AA}$).

Although the monatomic wire studied by Scлаuzero *et al.* are quite different from our current system, the inter-platinum-distances are comparable. Even more, in case of the NW2-geometry there are three Pt atoms (two on opposing sides of the trough, and the extra Pt atom in the trough) forming a mini monatomic wire spanning the trough, with three inequivalent adsorption sites located on it.

The adsorption site with the highest binding energy of all adsorption sites studied is the B1-site. In this case the CO molecule binds to two Pt atoms through a bridge configuration. The distance between the two Pt atoms is 2.682 \AA , slightly longer than the optimum inter-platinum-distance for a CO molecule adsorbed in a bridge configuration on a monatomic freestanding Pt

wire. The B2- and B3-sites have an ontop configuration, and are 0.43 eV and 0.25 eV lower in adsorption energy. This shows a nice qualitative agreement between this 3-atom monatomic Pt wire present in the NW2-system and a freestanding monatomic Pt wire.

For all adsorption sites studied on the NW2-surface, the CO bond lengths are only stretched slightly, 1.85 – 3.35%. Even more, comparing the values of r_{CO} and $r_{\text{C-surf}}$ with those found by Scлаuzero *et al.* shows perfect agreement for the CO bond length, and just fractionally larger lengths for the C-Pt distances in our embedded 3-atom Pt wire. This slightly larger length is a simple consequence of the Pt atoms being embedded in the NW2-surface. The B3-site is the only site where the CO molecule is perfectly perpendicular to the surface, this is due to the symmetry of the chemical environment. In contrast, the B2 adsorption site has a lower symmetry and the molecule bends along the asymmetry direction toward the 3-atom monatomic Pt wire.

Contrary to CO adsorbed on the NW1-surface, CO adsorbed on the NW2-surface seems much less destructive. This is because the NW dimers are anchored at their position by the presence of the extra Pt atom. Only CO adsorbed at the B1- or B3-site modifies the NW significantly. In both cases, the CO molecule has a bond to the extra Pt atom, weakening the bonds with the NW dimers. Furthermore, just as for the NW1-surface, the CO molecules are positioned between the NW dimers, pushing them outward, away from the molecule. The combination of these two effects is large enough to break the bonds between the NW dimers and the extra Pt atom. Due to the periodic boundary conditions and the size of our unit cell, the two NW dimers recombine to form a tetramer-chain between the two copies of the CO molecule. In contrast to the NW1-surface, the free NW dimers will not be able to block the next equivalent adsorption site due to the presence of a NW dimer anchored in place by its accompanying extra Pt atom.

IV. DISCUSSION

The results from the previous section show no clear-cut image for the CO adsorption system based solely on calculated energies, which might already be suspected from the history of CO adsorption on pure Pt surfaces. However, direct comparison with experiment is possible by means of calculated STM images. This method has already been shown very successful at identifying correct adsorption sites for CO, even when the calculated energies fail to do so.^{12,13} At the moment of writing only very little experimental work is available, and the actual underlying NW type is not always entirely clear. The earliest experimental work on this system, by Öncel *et al.*¹⁵, presents the adsorption of CO molecules on NWs separated 2.4 \AA , which based on our previous calculations (Ref. 19) leads to the assumption that these wires can be considered solitary NWs. In these experiments

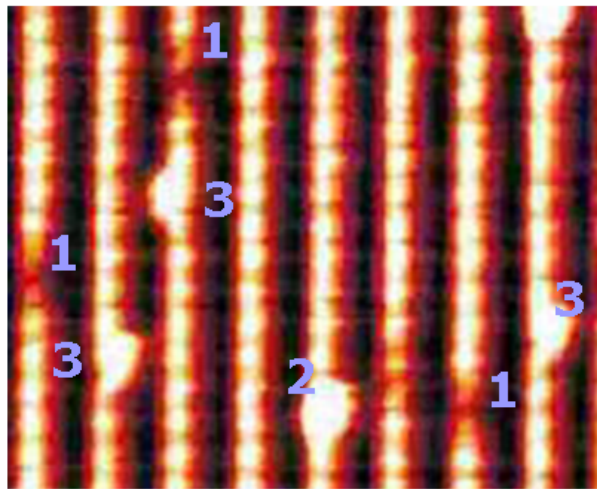


FIG. 3: (Color online) Zoom out of a section of figure 1 in Ref. 16, an empty state STM image (+1.8 V; 0.5 nA) of CO-decorated NWs, recorded at 77 K. We have indicated three CO adsorption sites. Site 1 shows a large depression in the wire. Sites 2 and 3 show large protrusions. In case of site 2 nicely centered on the NW, while for site 3 the protrusion is centered either left or right of the NW.

only one adsorption site was observed. It appears as a protrusion at negative bias, and as a depression at positive bias. Later work, by Kockmann *et al.*¹⁶, studied the adsorption of CO molecules on arrays of NWs spaced only 1.6 Å. Based upon the results presented in Ref. 19, we assume these wires to have a NW2-geometry. Unlike Öncel *et al.*, Kockmann and collaborators observed two adsorption sites, both different from the one observed by Öncel *et al.*

Based on this we will compare our results for solitary wires with the experiments of Öncel *et al.*, and those for array-NWs with the experiments of Kockmann *et al.*

A. CO adsorption on Pt induced nanowires

As reference images for the experiment we will use figure 2a and 2b of Ref. 15 for the solitary NWs and figure 1 of Ref. 16 for the NW arrays. Close examination of figure 1 in Ref. 16 shows three distinctly different adsorption sites, indicated in Fig. 3. Kockmann and collaborators on the contrary only identify two, considering sites 2 and 3 the same adsorption site. It is well known from literature that the electric field of the STM tip can influence the position and orientation of molecules adsorbed on a surface.³³ This can result in an extra broadening of the CO image along the scan lines.³⁴ This, however, can not cause the CO molecules at the adsorption site 2 in Fig. 3, to appear as site 3, since the latter is observed at both sides of the NW [*cf.* Fig. 3].

In addition to the formation and adsorption energies, STM images are calculated for all adsorption NW1-and

NW2-geometries. All NW1 CO-adsorption geometries show protrusions for both positive and negative simulated bias, with the exception of the A3a adsorption site. For the latter, a protrusion is visible in the filled state image [*cf.* Fig. 4c], while a depression is clearly present in the empty state image [*cf.* Fig. 4c]. The comparable A3b-structure on the other hand shows a clear protrusion on the adjacent quasi-dimer row (QDR) for all biases [*cf.* Fig. 4e]. However, this protrusion is not caused by the CO-molecule present, but by the Ge NW atom ejected from the trough instead [*cf.* Fig. 2b]. Removal of this Ge atom removes the protrusion and only a brightened Pt-Ge dimer, bound to the O atom, remains [*cf.* Fig. 4f]. The CO molecule itself remains invisible.

Of all adsorbed CO molecules only those on the A3 sites and on the Ge NW, are located “on” the NW. However, these are not the only CO molecules resulting in a CO-image “on” the wire. Due to the large tilt angle of the CO molecule at the A2-site the resulting image gives the impression of a CO molecule sitting, just slightly asymmetric, on top of the NW, as can be seen in Fig. 4a and 4b. For large negative bias the image is round, while becoming more and more bean-shaped for smaller negative biases and all positive biases.

CO molecules bound to Ge NW atoms show images which look bean-shaped for the A5 adsorption site, and two-lobbed donut-shaped for the A6 adsorption site.

Based on the adsorption energies found in Sec. III, the adsorption of CO on the Ge NW dimers can be excluded. Only the Pt adsorption sites near the NWs remain. For the solitary NWs the A3b-site can be excluded because for both positive and negative bias a depression is found, which is not reported in experiments.

The sites A1, A2, and A4 show a comparable behavior. Both in the filled and empty state pictures a large protrusion is clearly visible, slightly asymmetric to the NW position. Figures 4a and 4b show an A2 adsorbed CO molecule as example.

The A3a-site despite its low adsorption energy shows something interesting. The filled state picture shows a pear shaped image for the NW dimer [*cf.* Fig. 4c], just as was observed by Öncel *et al.*, and the empty state picture shows no NW dimer image [*cf.* Fig. 4d]. Comparison to figures 2a and b in Ref. 15 shows good agreement. Linescans along the NW for the A3a adsorption site, in comparison to a pristine NW are shown in Fig. 5. Due to periodic boundary conditions and the fact that our unitcell only contains 1 NW dimer, this image can only be used to compare to the region $\sim 0.5 - \sim 1.5$ nm in figure 3 of Ref. 15. Note that the linescans in figure 3 of Ref. 15 and Fig. 5 of this work are mirror images of each other (mirrored around the center of a NW dimer), indicating that the CO molecule was bound (the O-Ge bond) to the ‘left’ side of the NW dimer in experiment, while it is bound to the right side in our calculations [*cf.* Fig. 4c]. For the linescan of the filled state picture, the asymmetric shape and the width of the protrusion match

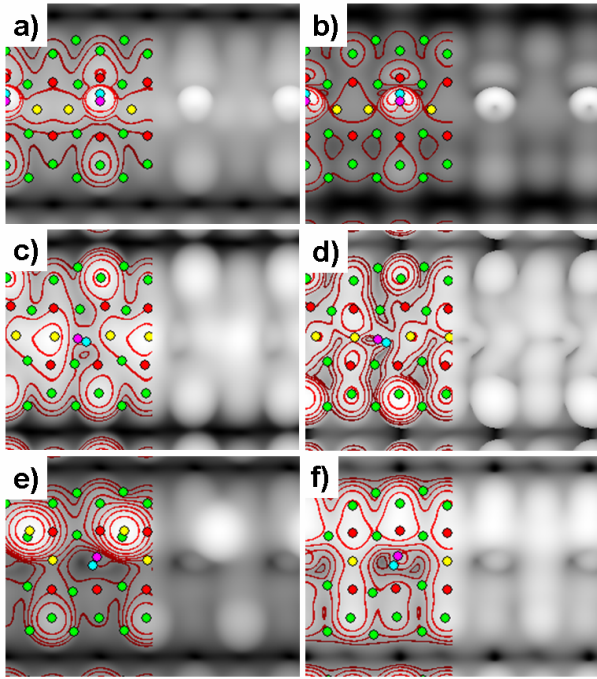


FIG. 4: (Color online) Calculated filled and empty state STM images for the A2 (filled (a) and empty (b)), A3a (filled (c) and empty (d)), A3b (filled (e)), and A3b1 (filled (f)) adsorption geometries. The simulated biases are for (a), (e), and (f) -1.50 V, (b) $+1.50$ V, (c) -0.70 V, (d) $+0.30$ V. Contours are added to guide the eye, they are separated 0.3 Å. Colored discs indicate atomic positions: green and red represent Ge and Pt atoms in the top two layers of the surface, yellow represent the Ge atoms forming the NW, and cyan and fuchsia represent the C and O atoms respectively.

very well. There is also a good agreement between the linescans of the empty state pictures. Note that in both cases the two small peaks have a different height, with the highest peak at the lower side of protrusion in the filled state picture. Furthermore, comparison to the linescan of a pristine NW shows the maximum of the filled state protrusion to be located near the center of the dimer, giving the impression that the CO molecule is located on top of the NW dimer in a bridge configuration (compare to figure 6.1b in Ref. 35). Also the location of the larger of the two small protrusions, in the empty state picture linescan, at the minimum between two NW dimers is in excellent agreement with the experimental observations (*cf.* figure 6.2b in Ref. 35). This shows that a CO molecule in between two NW dimers, bound to one NW dimer through the O atom, can look like a molecule bound on top of a NW dimer. The low binding energy found here remains problematic. However, the fact that taking into account the stretching of the molecule returns an energy comparable and better than most of the other adsorption structures could indicate the energy barrier for desorption to play an important role. This also indicates that for RT experiments where a much

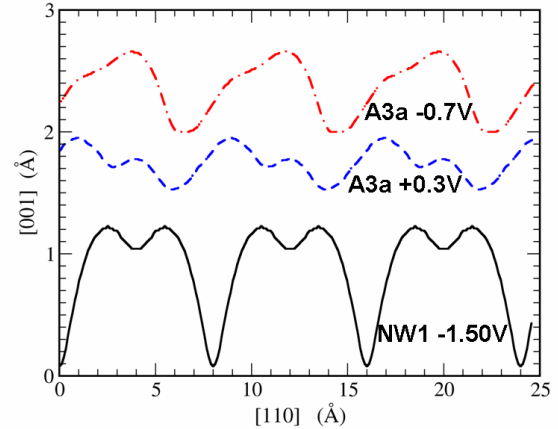


FIG. 5: (Color online) Linescan images along the NW for the clean NW at a simulated bias of -1.50 V (solid black curve), the CO molecule adsorbed at the A3a-site at a simulated bias of -0.70 V (dash-dotted red curve) and $+0.30$ V (dashed blue curve). For each system $z = 2.5$ Å is used to generate the calculated STM images from which the line scans are taken. The lines are shifted along the $[001]$ -axis.

lower CO density is present, reducing the contributions of direct and indirect interaction between CO molecules, this might not be as problematic. The good agreement of this structure with the experiment seems to support this idea.

Although Öncel *et al.* do not report observing any other adsorption sites, they do report the CO molecules to perform a 1D random walk along the NW. Since the A3a adsorption site does not easily allow for a CO molecule to just jump from one site to the next, some intermediate stable adsorption sites should be present to accommodate this mobility. Looking at the geometry of the relaxed structures a path can be imagined going from A3a to A2 [*cf.* Fig. 1a], by breaking the bond between the C atom and the Pt atom at the bottom of the trough and breaking the O-Ge bond. Rotation from the A2 to the A4 configuration and onto the A1 adsorption site, followed by the same path in reverse to the next A3a site. The binding energies of these three adsorption sites (A1, A2 and A4) differs only little making it an energetically possible path at RT.³⁶ These sites are also present on the NW2-surface, where the adsorption site B2 can be considered an alternative for the A2-site. The calculated STM images of the B2-site also show the same asymmetric protrusion in the filled and empty state pictures, while the adsorption energy (shown in Table III) lies in the range of the three A-sites. Site 3 in Fig. 3 clearly shows such an asymmetric adsorption site. Although the resolution in Fig. 3 is not sufficient to distinguish between the four adsorption sites mentioned above, it is sufficient to indicate their existence.

For the NW2-surface, the calculated STM images for the adsorption sites show quite a complex picture. The most simple behavior is observed for the B4-site. Both the filled and empty state pictures show, a round, slightly asymmetric CO image sticking out far above the surface and the NW. Conversely, a CO molecule at the B1-site shows a sharp round image which becomes smaller (even invisible) for biases close to the Fermi level [*cf.* Fig. 6a and 6b]. CO adsorbed at the B3 site, on the other hand, shows a nice round image for negative bias (*cf.* filled state picture in Fig. 6e), which becomes a two lobbed image for small positive bias but becomes invisible for large positive bias (*cf.* empty state picture in Fig. 6f).

In each of the above cases the CO image appears nicely centered on the NW, which can be understood from the underlying geometry. In case of a CO molecule adsorbed at the B2-site, the tilting of the molecule over the trough causes the CO image to appear only slightly shifted away from the center of the NW, giving the impression the CO molecule might be located on the wire itself [*cf.* Fig. 6c and 6d]. Both the filled and empty state pictures show nice elliptical CO images for large biases, while close to the Fermi level the elliptical image becomes two-lobbed. As with all the previous cases where a donut or two-lobbed CO image was observed, this are the π -orbitals of the molecule that are being observed.¹²

The only adsorption site left to discuss, is the B5-site. Here the CO molecule bridges the entire trough, so a serious modification of the calculated STM pictures might be expected. Amazingly, the calculated STM images show *nothing*. Both for filled and empty state pictures a normal NW image is observed, and not even the slightest indication of the CO molecules presence can be observed, making the CO molecule effectively *invisible*.

Figure 6 shows the calculated STM images for B1, B2, and B3 adsorbed CO molecules. When comparing these images with experimental STM images, there are a few things we need to keep in mind. i) The way the STM images were calculated. By using a point source as tip, almost infinitely sharp images are obtained, while in reality tip-size and geometry will influence the obtained STM image. This will mainly manifest itself in a broadening of the observed features. ii) No dynamic tip-substrate interactions are included in the calculated STM images. Although for a clean surface the effect of the tip on the surface geometry is almost negligible, this is not the case for a molecule bound to the surface.³³ At low coverage, molecules retain a large freedom to move, even if their anchor point remains fixed, resulting in a blurring of their observed STM image. iii) The position of the molecular orbitals, especially the states above the Fermi level are not that well described in DFT (this is the well known band gap problem). This means that it is not always possible to use the same simulated bias as the experimental one. Points i and ii explain why the CO images in Fig. 3

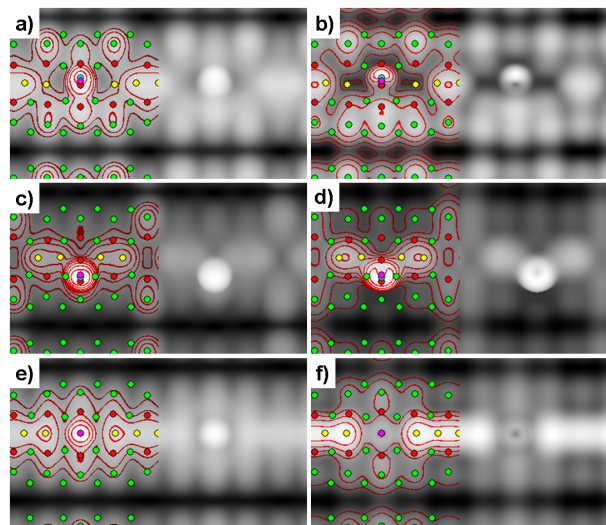


FIG. 6: (Color online) Calculated STM images of CO molecules adsorbed at the B1- (a and b), B2- (c and d) and B3-sites (e and f). The distance above the highest atom was chosen $z = 2.0$ Å. Filled state images (a), (c) and (e) are at a simulated bias of -1.80 V, while for the empty state images (d) and (f) a simulated bias of $+1.80$ V was used. For the empty state image (b) a simulated bias of $+1.50$ V was used. Contours are added to guide the eye. All contours are separated 0.2 Å in the z direction. Colored discs indicate the atom positions in the top layers. Ge and Pt atoms in the two top layers are shown in green and red respectively. Yellow discs are used to indicate the Ge NW atoms, while cyan and fuchsia is used for the C and O atoms respectively.

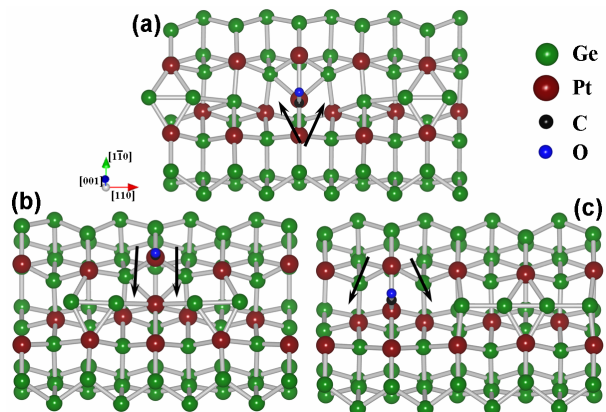


FIG. 7: (Color online) Ball-and-stick representation of the relaxed geometries of CO molecules adsorbed at sites B1 (a), B2 (b) and B3 (c). Arrows indicate broken bonds between the Ge NW atoms and the extra Pt atom for the B1 (a) and B3 (c) adsorption sites. For the B2 adsorption site (b) these bonds, indicated with the arrows, are not broken.

show up to be sometimes two dimers long with a width larger than that of the NW.

With this in mind, the three adsorption sites shown

in Fig. 3 can be identified by comparing the calculated empty and filled state pictures to experimental STM pictures. Site 1 shows a depression in the empty state picture, centered between two NW dimers. The filled state pictures on the other hand show a small protrusion.¹⁶ Figures 6e and 6f show the same behavior for the B3 adsorbed CO molecule. Its geometry, shown in Fig. 7c, shows the CO molecule bound in an on-top configuration to the extra Pt atom. This bond weakens the bonds between the extra Pt atom and the NW dimers, allowing for the presence of the CO molecule to break them entirely, pushing the two NW dimers away from the CO molecule. The limited size of the surface cell and the periodic boundary conditions results in the formation of a Ge tetramer, and a limitation of the length of the depression to roughly 5–6 Å. In experiment however the NW dimers could be pushed even further apart resulting in a large gap around the CO molecule, which explains the experimentally observed length of the depression to be roughly two dimer lengths. The lack of small depressions on either side of the CO molecule in the experimental filled state pictures can be understood as a consequence of the molecule-tip interactions mentioned earlier.

The second site seen in Fig. 3, shows a protrusion in both filled and empty state pictures. Figures 3a and b in Ref. 16 also show that the relative height with regard to the NW is smaller in the empty state picture than in the filled state picture. This turns out to be in agreement with the images found for the B1 adsorbed CO molecule [*cf.* Fig. 6a and 6b]. At this adsorption site the CO molecule is bound in a bridge configuration to the extra Pt atom and a Pt atom of the surface dimer row [*cf.* Fig. 7a]. Again the bond with the extra Pt atom allows for the bonds between the NW dimers and the extra Pt atom to be broken, and the NW dimers to move away from the CO molecule resulting in a large gap around the CO molecule. Table III shows this bridge configuration to have the highest adsorption energy, in agreement with the *ab initio* calculations of Sclauzero *et al.*¹⁷

The third and last adsorption site indicated in Fig. 3 shows a clearly asymmetric protrusion in the empty states picture. Unfortunately no experimental filled state pictures have been published for this adsorption site, but based on all the other adsorption sites observed in experiment we will assume that also in this case a protrusion is observed in the filled state image. Figures 6c and 6d, show the filled and empty state pictures of a CO molecule adsorbed at site B2. This CO molecule is bound to a Pt atom in the surface dimer row, see Fig. 7b. Because it is tilted toward the NW, the resulting image appears just slightly asymmetric of the NW, making it a very good candidate for the adsorption site 3 indicated in Fig. 3. In combination with the adsorption sites A1, A2, and A4, this adsorption site gives a possible migration path for the mobility observed by Öncel *et al.*¹⁵

In their investigation of CO adsorption on the Pt induced NWs Kockmann *et al.* also observe a, what they call, *remarkably long-ranged repulsive interaction*

between the CO molecules. This repulsion, they found, has a range up to 3–4nm (or 4–5 NW dimers) along the NW direction. Due to its long range they concluded that this repulsive interaction can not just be a mere electrostatic repulsion. Furthermore, Kockmann *et al.* note that the characteristic long-ranged repulsive interaction is independent of the adsorption sites involved. This long range interaction along the NW is sharp contrast with the fact that no significant interaction is observed between CO molecules on adjacent wires. This means the origin of the repulsive interaction needs to be linked to the NW itself. We have shown for the adsorption sites on the NW1- and the NW2-surface that the presence of CO molecules modifies the nearby NW dimers in varying degrees. When the CO molecule is located between NW dimers (*e.g.* A3, B1, and B3) it seems to repel the nearby NW dimers. For example, for the A3-site we find the resulting modifications to extend up to two NW dimers in each direction. Two other examples are shown in Fig. 7a and c. They show the interaction between two periodic copies of a CO molecule on the NW2-surface. These copies are separated 2 NW dimer apart and can press their neighboring NW dimers toward one-another far enough such that they form a tetramer. This effectively results in an indirect interaction between the two CO molecules. The surface strain mediating the indirect CO interaction is directed purely along the NW itself. The NW dimers which are pressed away from their original position will in their turn press further neighboring NW dimers from their equilibrium position and so on. These dislocated NW dimers block the possible adsorption sites resulting in an effective long range repulsive interaction.

As a final remark in this paragraph, we would like to point out the B5 adsorption configuration. Its high adsorption energy (only 140 meV below that of the B1 configuration) makes it also a reasonable adsorption configuration. Figures 8a and 8b show the calculated filled and empty state pictures. These show the CO molecule to be invisible, while the rest of the NW image remains unchanged. This is also the case for other simulated biases (± 0.30 and ± 0.70 eV), leading to the conclusion that this adsorption configuration could well be present in experiment, but invisible for STM. Only high resolution linescans orthogonal to the NWs at the position indicated in Fig. 8a could show the induced asymmetry of the QDRs [*cf.* Fig. 10], possibly combined with the observation that these asymmetric linescans are on average lower than those symmetric ones on locations where no CO molecule is present. Another option one could imagine to make the CO molecule appear, is by breaking its O-Pt bond with a small current surge through the STM tip. The CO molecule might then revert to the B2 adsorption configuration, which would be clearly visible in both filled and empty state pictures [*cf.* Fig. 6c and 6d].

This was for the case where the substrate is a NW array. For solitary NWs, which we have already shown to be less stable under CO adsorption, observation might

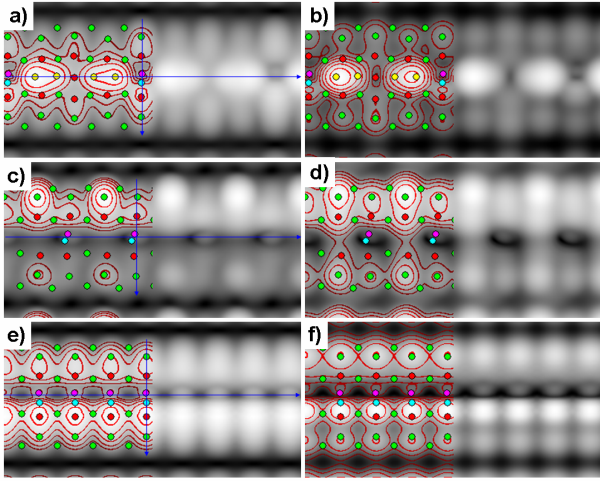


FIG. 8: (Color online) Calculated STM images of CO molecules adsorbed in bridging configurations B5 (a and b), A3b2 (c and d) and A7₂CO (e and f). The distance above the highest atom was chosen $z = 2.0$ Å. Filled state pictures (a), (c) and (e) are at a simulated bias of -1.50 V, while for the empty state pictures (b), (d) and (f) a simulated bias of $+1.50$ V is used. Contours are added to guide the eye, and are separated 0.2 Å. Colored discs indicate the atom positions in the top layers. Ge and Pt atoms in the two top layers are shown in green and red respectively. Yellow discs are used to indicate the Ge NW atoms, while cyan and fuchsia is used for the C and O atoms respectively. Blue arrows show the position and direction of the linescans shown in Fig. 10

be a little bit easier. Table IV shows the A7 configuration (*cf.* Fig. 9b, it is the analog of the B5 configuration) to have a very high adsorption energy. Here the steric repulsion between the CO molecule and the NW dimers will create a hole in the NW centered around the CO molecule. This defect should show up as a depression over a wide range of biases. This wide depression would have a small protrusion in its center and a width of at least 8 Å.³⁷

B. Molecular electronics on Pt modified Ge(001)?

From these calculations and the experiments presented in literature, the possible application of this system for 1D molecular electronics becomes very unlikely. The long-ranged interaction observed by Kockmann *et al.* and its explanation in light of the calculations performed in this work, seems to be the main problem.

Up to this point we mainly focussed on identifying the experimentally observed structures. The B5 adsorption configuration, and the comparable A3b configuration have not yet been discussed in light of experiments, while showing almost the best adsorption energies. The calculated STM images for these structures show something very peculiar: the total lack of an image for the CO molecule. In case of the A3b adsorption site a

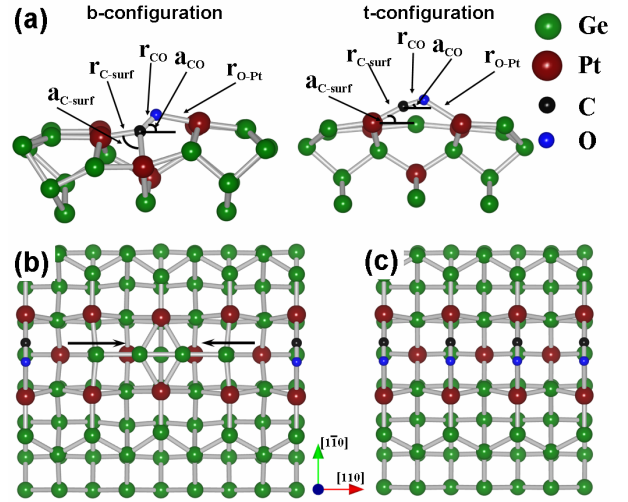


FIG. 9: (Color online) (a) Ball-and-stick representation of the two bridging CO configurations. Geometrical parameters given in Table IV are indicated. Ball-and-stick representation of the A7 (b) and A7₂CO (c) structures. Arrows in (b) show the drift direction of the NW dimers.

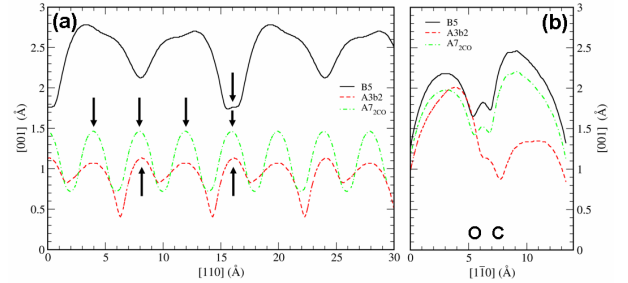


FIG. 10: (Color online) Calculated linescan images along (a) and orthogonal (b) to the trough/NW for the B5 (solid black curve), the A3b2 (red dashed curve) and the A7₂CO (green dash-dot curve) configuration. The linescans are taken along the arrows shown in Fig. 8 (a), (c), and (e). The arrows in (a) indicate the positions of the CO molecules, while C and O show the positions of the C and O atom in (b).

large protrusion is still visible, however this is an ejected Ge atom of the NW dimer [*cf.* Fig. 2b]. This ejection was due to the limited unitcell size. The steric repulsion between two periodic copies of the CO molecule and the single Ge NW dimer prohibited the Ge dimer to be displaced sufficiently along the NW direction. To remove this ‘computational artefact’ the ejected Ge atom is removed (A3b1), and in a second calculation both Ge atoms forming the NW dimer are removed (A3b2). Also an adsorption structure with B5 configuration on a NW1 surface is build (A7), using a double NW1 surface cell. Table IV shows the formation and adsorption energies for these new structures in comparison to the B5- and A3b-structures. Removal of the Ge NW atoms

**Adsorption energies and geometrical parameters for bridging CO molecules
on a Pt modified Ge(001) surface.**

	E_f (eV)	E_{ad} (eV)	coord.	r_{CO} (Å)	a_{CO} (°)	r_{C-surf} (Å)	a_{C-surf} (°)	r_{O-Pt} (Å)
NW1 A3b	-1.485	-2.069	b	1.214	47	2.012 (2.066)	101	2.249
NW1 A3b1	-1.163	-2.276	b	1.207	43	1.960 (2.106)	90	2.167
NW1 A3b2	0.390	-2.094	b	1.204	44	1.964 (2.084)	87	2.190
NW2 B5	-0.784	-2.197	t	1.170	20	1.883	28	2.433
NW1 A7	-1.589	-2.361	t	1.169	17	1.884	28	2.401
NW1 A7 _{2CO}	-3.741	-2.214	t	1.167	19	1.882	27	2.394

TABLE IV: Formation and adsorption energies for CO adsorbed in configurations bridging the trough between two neighboring QDRs. Adsorption sites are shown in Fig. 9a. The B5 and A3b values are duplicated from Table I for ease of comparison. r_{CO} , r_{C-surf} , and r_{O-Pt} are the C-O, C-Pt and O-Pt bond lengths, the value between brackets for r_{C-surf} is the bond length of the C atom to the Pt atom at the bottom of the trough. a_{CO} and a_{C-surf} are the bond angles with regard to the surface plane. In case of bridge adsorption a_{C-surf} is the angle between the two C-surface bonds.

clearly decreases the formation energy of the surface, which is due to the uncovering of the imbedded Pt atoms.¹⁹ The adsorption energy of the CO molecule however remains roughly the same. Also the geometrical parameters barely change. The bond lengths decrease slightly, due to the reduced steric repulsion between the CO molecules and the Ge dimer atoms, moving the CO molecule closer to the surface.

In case of the A7 adsorption configuration, the lack of anchor point for the NW dimers causes them to drift away from the CO molecule due to the steric repulsion. Which, because of the limited unit cell size, results in the formation of a Ge tetramer as is shown in Fig. 9b. The geometric parameters for the CO molecules in the B5 and A7 adsorption configurations are almost identical. However, the distance between a CO molecule and the nearest Ge atom of a NW dimer is approximately 4.3 Å in case of the A7 configuration, while it is only 3.3 Å in case of the B5 configuration. This indicates the improvement in adsorption energy, going from the B5 to the A7 configuration, can be attributed to the reduction of the steric repulsion between the CO molecule and the Ge NW dimers.

Because uncovering the imbedded Pt atoms has a negative influence on the formation energy, a model is build with the entire NW removed and replaced by a maximum coverage of CO molecules in an A7 configuration (A7_{2CO}). The A7_{2CO} structure contains two CO molecules per 4×2 surface cell [*cf.* Fig. 9c], making this a four times higher coverage than the A7 case. A large increase in the formation energy is found, while the steric repulsion only has a minute influence on the adsorption energy of the CO molecules. Furthermore, the geometrical parameters remain almost unchanged making this, from the geometrical point of view, a very good candidate for 1D molecular electronics. However, one small problem remains: these CO molecules in either b or t bridging configuration are invisible in STM.

Figure 8 shows both filled and empty state pictures of the B5, A2b2, and A7_{2CO} adsorption geometries. For the B5 adsorption configuration the linescan (black solid line shown in Fig. 10) is almost unmodified compared to the linescan of the pristine NW. The only modification is found in the line scan orthogonal to the trough/NW. In case of a t bridging configuration, the dimer of the QDR which is bound to the C atom is higher than the dimer bound to the O atom, while the opposite is true for the b bridging configuration.

In conclusion, if one would succeed in stripping away the Ge NW without damaging the underlying substrate, a high coverage of CO molecules in bridging configuration could be recognized by this asymmetry in the QDR images. The formation and adsorption energies are highly favorable, making this also energetically an interesting template for 1D molecular electronics.

V. CONCLUSIONS

In this paper we have studied the adsorption of CO molecules on Pt induced NWs on Ge(001) using *ab initio* DFT calculations. We show CO has a strong preference for adsorption on the Pt atoms imbedded in the Ge(001) surface. As a consequence CO molecules do not bind directly on top of the Ge dimers forming the NWs, contrary to the experimental assumptions. By direct comparison of calculated STM images to experimental STM images we have successfully identified the observed adsorption sites. We have shown that the Pt atoms lining the troughs in which the Ge NWs are imbedded provide the necessary adsorption sites to explain all experimentally observed CO adsorption sites.

CO molecules in ontop configurations next to the NW tilt toward it, presenting STM images located on the NW. CO molecules bound in between NW dimers, with the O

atom also bound to a Ge NW dimer modify the electronic structure of this Ge atom sufficiently to give the appearance of a protrusion on this Ge dimer. This gives rise to the short-bridge CO adsorption site observed by Öncel *et al.* A CO molecule bound in an atop configuration on the extra Pt atom of the NW2-surface, showing a protrusion at negative bias and a depression at positive bias, is found to show good agreement with the experimentally observed long-bridge site, seen by Kockmann *et al.* The short-bridge site observed by this group is identified as a CO molecule in a bridge configuration in between NW dimers.

A path for mobility along the wire is presented, showing the CO molecule to move along the Pt atoms of the underlying QDRs. The long-ranged interaction observed by Kockmann *et al.* is explained through the dislocation of NW dimers, in the vicinity of the CO molecule. These dislocated NW dimers in turn block the nearby CO-adsorption sites.

We also predict the presence of invisible bridging CO

molecules, and present methods for observing them experimentally. Also the possibility of 1D molecular electronics is touched. After removal of the Ge NW dimers, stable, invisible wires of parallel CO molecules, along the Pt lined troughs, can be obtained. This configuration has a large formation energy $E_f = -3.74$ eV and an adsorption energy per CO molecule $E_{ad} = -2.21$ eV at maximum CO coverage.

Acknowledgements

This work is part of the research program of the “Stichting voor Fundamenteel Onderzoek der Materie” (FOM) and the use of supercomputer facilities was sponsored by the “Stichting Nationale Computer Faciliteiten” (NCF), both financially supported by the “Nederlandse Organisatie voor Wetenschappelijk Onderzoek” (NWO).

-
- * Current Affiliation: Department of Inorganic and Physical Chemistry, Ghent University, Krijgslaan 281 - S3, 9000 Gent, Belgium; email: dannyvanpoucke@gmail.com; URL: <http://users.ugent.be/~devpouck/>
- ¹ A. Eichler, Surf. Sci. **498**, 314 (2002).
 - ² R. Imbihl and G. Ertl, Chem. Rev. **95**, 697 (1995).
 - ³ G. Ertl, M. Neumann, and K. M. Streit, Surf. Sci. **64**, 393 (1977).
 - ⁴ H. Froitzheim, H. Hopster, H. Ibach, and S. Lehwald, Appl. Phys. **13**, 147 (1977).
 - ⁵ H. Steininger, S. Lehwald, and H. Ibach, Surf. Sci. **123**, 264 (1982).
 - ⁶ D. F. Ogletree, M. A. V. Hove, and G. A. Somorjai, Surf. Sci. **173**, 351 (1986).
 - ⁷ Y. Y. Yeo, L. Vattuone, and D. A. King, J. Phys. Chem. **106**, 392 (1997).
 - ⁸ P. J. Feibelman, B. Hammer, J. K. Norskov, F. Wagner, M. Scheffler, R. Stumpf, R. Watwe, and J. Dumesic, J. Phys. Chem. B **105**, 4018 (2001), and references herein.
 - ⁹ P. van Beurden, H. G. J. Verhoeven, G. J. Kramer, and B. J. Thijsse, Phys. Rev. B **66**, 235409 (2002).
 - ¹⁰ M. Alaei, H. Akbarzadeh, H. Gholizadeh, and S. de Gironcoli, Phys. Rev. B **77**, 085414 (2008).
 - ¹¹ I. Dabo, A. Wieckowski, and N. Marzari, J. Am. Chem. Soc. **129**, 11045 (2007).
 - ¹² M. L. Bocquet and P. Sautet, Surf. Sci. **360**, 128 (1996), ISSN 0039-6028.
 - ¹³ M. Ø. Pedersen, M.-L. Bocquet, P. Sautet, E. Lægsgaard, I. Stensgaard, and F. Besenbacher, Chem. Phys. Lett. **299**, 403 (1999).
 - ¹⁴ O. Gürlü, O. A. O. Adam, H. J. W. Zandvliet, and B. Poelsema, Appl. Phys. Lett. **83**, 4610 (2003).
 - ¹⁵ N. Öncel, W. J. van Beek, J. Huijben, B. Poelsema, and H. J. W. Zandvliet, Surf. Sci. **600**, 4690 (2006).
 - ¹⁶ D. Kockmann, B. Poelsema, and H. J. W. Zandvliet, Phys. Rev. B **78**, 245421 (2008).
 - ¹⁷ G. Sciauzero, A. D. Corso, A. Smogunov, and E. Tosatti, Phys. Rev. B **78**, 085421 (2008).
 - ¹⁸ D. E. P. Vanpoucke and G. Brocks, Phys. Rev. B **77**, 241308 (2008).
 - ¹⁹ D. E. P. Vanpoucke and G. Brocks, Phys. Rev. B **81**, 085410 (2010).
 - ²⁰ K. Fukutani, T. T. Magkoev, Y. Murata, M. Matsumoto, T. Kawauchi, T. Magome, Y. Tezuka, and S. Shin, J. Electron Spectrosc. Relat. Phenom. **88**, 597 (1998).
 - ²¹ P. E. Blöchl, Phys. Rev. B **50**, 17953 (1994).
 - ²² G. Kresse and D. Joubert, Phys. Rev. B **59**, 1758 (1999).
 - ²³ G. Kresse and J. Hafner, Phys. Rev. B **47**, 558 (1993).
 - ²⁴ G. Kresse and J. Furthmüller, Phys. Rev. B **54**, 11169 (1996).
 - ²⁵ H. J. Monkhorst and J. D. Pack, Phys. Rev. B **13**, 5188 (1976).
 - ²⁶ J. Tersoff and D. R. Hamann, Phys. Rev. B **31**, 805 (1985).
 - ²⁷ The NW at the edge of a NW array next to bare β -terrace, just like a solitary NW, does not present the 4×1 periodicity typical for NWs in a NW-array. It was argued in Ref. 19 that these edge NWs might have the same geometry as the solitary NWs. The latter could be understood to be an extreme case of a NW array, *i.e.* one only consisting of its edge. Because of this, we will refer to both solitary and edge NWs as solitary NWs, while array NWs refers to the none-edge NWs of a NW array.
 - ²⁸ A. van Houselt, T. Gnielka, J. M. J. Aan de Brugh, N. Öncel, D. Kockmann, R. Heid, K. P. Bohnen, B. Poelsema, and H. Zandvliet, Surf. Sci. **602**, 1731 (2008).
 - ²⁹ O. R. Gilliam, C. M. Johnson, and W. Gordy, Phys. Rev. **78**, 140 (1950).
 - ³⁰ R. Hirschl, F. m. c. Delbecq, P. Sautet, and J. Hafner, Phys. Rev. B **66**, 155438 (2002).
 - ³¹ D. E. P. Vanpoucke and G. Brocks, MRS 2009 spring meeting **symposium Z**, 6 (2009), submitted.
 - ³² Two surface unit cells are shown in Fig. 2b.
 - ³³ M. M. D. Ramos, A. P. Sutton, and A. M. Stoneham, J. Phys.: Condens. Matter. **3**, S127 (1991).
 - ³⁴ This means orthogonal to the NWs in the cited experimental pictures.

³⁵ N. Öncel, Ph.D. thesis, University of Twente (2007).

³⁶ The computational cost to calculate diffusion barriers between these intermediate steps is, due to the system size, too large.

³⁷ In our limited surface cell the NW dimers could not spread further before colliding with periodic copies, limiting the width of the depression to $\sim 8 \text{ \AA}$.